

## **FOLLOW-UP RESPONSES TO REVIEWER #2**

Ms. Ref. No.: Atmos. Chem. Phys. Discuss., doi:10.5194/acp-2018-556.

Title: Nitrogen oxides in the global upper troposphere: interpreting cloud-sliced NO<sub>2</sub> observations from the OMI satellite instrument

Journal: Atmos. Chem. Phys. Discuss.

Reviewer comments are in blue. Responses are in black and include line numbers consistent with the updated manuscript with changes tracked (response to reviewer #2 and minor editorial updates). The manuscript starts on the 4<sup>th</sup> page of this pdf.

### **Responses to Anonymous Referee #1:**

We would like to thank reviewer #2 for their second meticulous review of the paper. Their comments and careful thought of the paper are incredibly helpful and will no doubt improve the quality of the publication.

*1. line 60: Bucsela et al. (2010) should appear on the previous line.*

Updated.

*2. lines 99 -100: I still do not understand how taking the difference between the column covering 380 hPa and the tropopause and that covering 380 to 500 hPa yields the column centered at 380 hPa (330 - 450 hPa).*

We now clarify that UT NO<sub>2</sub> is obtained as the difference between two neighboring partial tropospheric columns retrieved above clouds that are at a mean pressure range of 330-450 hPa and 380-500 hPa (lines 99-100).

*3. line 107: The criterion of cloud radiance fraction > 0.7 allows some amount of signal from the lower troposphere to enter the cloud-sliced data set. Both Choi et al. (2014) and Pickering et al. (2016) favored CRF > 0.9 for this reason. Pickering et al. (2016) report a 5% high bias when using CRF >0.7 compared with CRF > 0.9. A paragraph is needed discussing all of the uncertainties involved in the OMI cloud-sliced NO<sub>2</sub> product including this possible bias.*

Thank you for highlighting the sensitivity test by Pickering et al. (2016). Their results clearly demonstrate that the effect of different CRF thresholds of 0.9 and 0.7 is small (<5%) and not significant (derived NO<sub>x</sub> yields have large variability: 117 ± 94 mol fl<sup>-1</sup> using a CRF>70% and 112 ± 67 mol fl<sup>-1</sup>). We now state this in the paper (lines 117 and 128-127).

*4. lines 257 - 262: The production rate derived here is very model dependent. The authors need to state this fact and that the values derived here are influenced by any error that exists in the UT NO<sub>y</sub> chemistry that may be in GEOS-Chem. Such possible errors have recently been discussed by Travis et al. (2016) and Silvern et al. (2018).*

We now state that the modelled and observed NO<sub>2</sub> are consistent over the pressure range of the OMI UT NO<sub>2</sub> product (6-9 km). The comparison between modelled and observed NO<sub>2</sub> by Silvern et al. (2018) is adapted in Figure 1 below and shows that the model reproduces the observed NO<sub>2</sub> across the altitude range of the OMI UT NO<sub>2</sub> product (lines 225-227). The bias reported by Travis and Silvern is for higher altitudes.

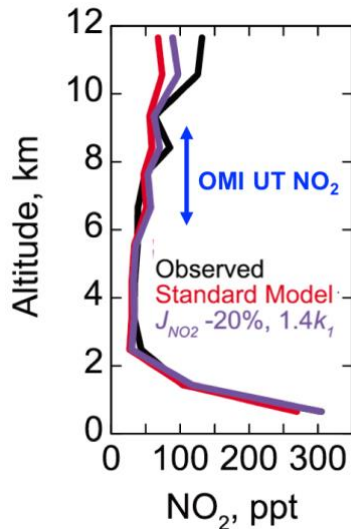


**Figure 1.** Comparison of TD-LIF and GEOS-Chem  $\text{NO}_2$  during SEAC<sup>4</sup>RS (adapted from Silvern et al., 2018). Two versions of GEOS-Chem are shown that test sensitivity of  $\text{NO}_2$  vertical distribution to uncertainties in reaction kinetics and photolysis. Blue arrow shows the altitude range of the NASA OMI UT  $\text{NO}_2$  product.

5. page 3, line 97: *Is aerosol really accounted for in the  $\text{NO}_2$  air mass factors, and if so, how?*

*Yes. We now reference Boersma et al. (2004) (line 122) that is in turn referenced by Belmonte-Rivas et al. (2015) when describing the air mass factor calculation.*

*I disagree. Please have another look at Boersma et al., 2004 last sentence of section 3.2. Aerosols are not explicitly taken into account in the DOMINO  $\text{NO}_2$  data product, only implicitly in partially cloudy scenes through the cloud correction applied. However, this correction has no effect on the cloudy scenes discussed here.*

Thank you for pointing us to the appropriate location in Boersma et al. (2004) that makes clear that aerosols are not directly accounted for in the DOMINO  $\text{NO}_2$  AMF calculation. We have updated the text to reflect this (line 95).

6. page 7, line 199: *I understand that aircraft measurements are screened for stratospheric air masses in tropospheric applications. However, here data are compared to satellite retrievals, and these will -- as far as I understand -- include such stratospheric air masses if they are in the right pressure range above a cloud. I therefore wonder if this screening really makes sense here.*

*Both the aircraft and satellite products exclude stratospheric contributions, and so the comparison is consistent. We now clarify that the OMI satellite product is tropospheric  $\text{NO}_2$  only (line 74). We already state that the KNMI product removes stratospheric  $\text{NO}_2$  by subtracting the stratospheric contribution in the retrieval (lines 121-122). We now elaborate that the stratospheric contribution in the NASA product is removed when differencing two nearby partial columns, as  $\text{NO}_2$  aloft is assumed uniform (lines 134-135 and lines 141-142).*

*This is not the point. The NASA product takes the difference in  $\text{NO}_2$  columns over neighbouring clouds having different cloud top. Any  $\text{NO}_2$  in between these altitudes will contribute to the retrieved UT mixing ratio, regardless of its origin. If stratospheric  $\text{NO}_2$  is brought down to the UT, the cloud slicing method will detect it as UT  $\text{NO}_2$  (as it should).*

The retrieval approach of Choi et al. (2014) only considers scenes with well-mixed NO<sub>2</sub>, diagnosed with a vertical gradient threshold of 0.33 pptv hPa<sup>-1</sup> from the GMI chemical transport model. We also only consider scenes with more than 50 measurements at coarse resolution (5° × 8°), so downwelling from the stratosphere that concerns the reviewer would have to persist throughout the gridsquare and over the whole season for multiple years (2005-2007) to bias the OMI UT NO<sub>2</sub>. We also now state that the contribution of stratospheric injection, as estimated by Murray et al. (2012) using GEOS-Chem, is small (lines 240-242).

*7. Please add the uncertainty estimates for the NO<sub>x</sub> yield and global lightning NO<sub>x</sub> source given in the text also to the abstract and conclusions.*

The error in the NO<sub>x</sub> yield and global lightning NO<sub>x</sub> source is now stated in the Abstract and Conclusions. We have also included the estimate of global lightning NO<sub>x</sub> with the size of the uncertainty inferred from the relative size of the uncertainty in the NO<sub>x</sub> production rate (lines 286-289).

### **References:**

Murray et al. (2012), doi:10.1029/2012jd017934.

# Nitrogen oxides in the global upper troposphere: interpreting cloud-sliced NO<sub>2</sub> observations from the OMI satellite instrument

Eloise A. Marais<sup>1,2,\*</sup>, Daniel J. Jacob<sup>2,3</sup>, Sungyeon Choi<sup>4</sup>, Joanna Joiner<sup>4,5</sup>, Maria Belmonte-Rivas<sup>6</sup>, Ronald C. Cohen<sup>7,8</sup>, Steffen Beirle<sup>9</sup>, Lee T. Murray<sup>10</sup>, Luke D. Schiferl<sup>11,\*\*</sup>, Viral Shah<sup>12</sup>, Lyatt Jaeglé<sup>12</sup>

5 <sup>1</sup>School of Geography, Earth, and Environmental Sciences, University of Birmingham, Birmingham, UK.

<sup>2</sup>John A Paulson School of Engineering and Applied Sciences, Harvard University, Cambridge, MA, USA.

<sup>3</sup>Earth and Planetary Sciences, Harvard University, Cambridge, MA, USA.

<sup>4</sup>Science Systems and Applications Inc., Lanham, MD.

<sup>5</sup>NASA Goddard Space Flight Center, Greenbelt, MD.

10 <sup>6</sup>Royal Netherlands Meteorology Institute, De Bilt, the Netherlands.

<sup>7</sup>Department of Chemistry, University of California at Berkeley, Berkeley, CA.

<sup>8</sup>Department of Earth and Planetary Science, University of California at Berkeley, Berkeley, CA.

<sup>9</sup>Max-Planck-Institut für Chemie, Mainz, Germany.

<sup>10</sup>Department of Earth and Environmental Sciences, University of Rochester, Rochester, New York, USA.

15 <sup>11</sup>Department of Civil and Environmental Engineering, Massachusetts Institute of Technology, Cambridge, USA.

<sup>12</sup>Department of Atmospheric Sciences, University of Washington, Seattle, WA, USA.

\* Now at: Department of Physics and Astronomy, University of Leicester, Leicester, UK.

\*\* Now at: Lamont-Doherty Earth Observatory, Columbia University, Palisades, NY, USA.

Correspondence to: Eloise A. Marais (eloise.marais@le.ac.uk)

20 **Abstract.** Nitrogen oxides (NO<sub>x</sub> ≡ NO + NO<sub>2</sub>) in the upper troposphere (UT) have a large impact on global tropospheric ozone and OH (the main atmospheric oxidant). New cloud-sliced observations of UT NO<sub>2</sub> at 450-280 hPa (~6-9 km) from the OMI satellite instrument produced by NASA and KNMI provide global coverage to test our understanding of the factors controlling UT NO<sub>x</sub>. We find that these products offer useful information when averaged over coarse scales (20° × 32°, seasonal), and that the NASA product is more consistent with aircraft observations of UT NO<sub>2</sub>. Correlation with LIS/OTD satellite observations of lightning flash frequencies suggests that lightning is the dominant source of NO<sub>x</sub> to the upper troposphere except for extratropical latitudes in winter. [The NO<sub>2</sub> background in the absence of lightning is 10-20 pptv.](#) We infer a global mean NO<sub>x</sub> yield of 280 ± 80 moles per lightning flash, with no significant difference between the tropics and mid-latitudes, and a global lightning NO<sub>x</sub> source of 5.9 ± 1.7 Tg N a<sup>-1</sup>. There is indication that the NO<sub>x</sub> yield per flash increases with lightning flash footprint and with flash energy.

## 1. Introduction

30 Nitrogen oxides (NO<sub>x</sub> ≡ NO + NO<sub>2</sub>) in the upper troposphere (UT) have profound effects on the oxidizing capacity of the atmosphere and on climate, but the factors controlling their concentrations are poorly understood. NO<sub>x</sub> in the UT impacts climate by efficiently producing ozone where it is a potent greenhouse gas (Dahlmann et al., 2011; Worden et al., 2011; Rap et al., 2015) and by increasing the concentration of OH (the main tropospheric oxidant) (Murray et al., 2012; Murray et al., 2014). Primary NO<sub>x</sub> sources in the UT include lightning, aircraft, convective injection, and downwelling from the stratosphere (Ehhalt et al., 1992; Jaeglé et al., 1998; Bertram et al., 2007). NO<sub>x</sub> cycles chemically with reservoir species including nitric acid (HNO<sub>3</sub>), pernitric acid (HNO<sub>4</sub>), dinitrogen pentoxide (N<sub>2</sub>O<sub>5</sub>), peroxyacetylnitrate (PAN), and other organic nitrates, thus defining the NO<sub>y</sub> chemical family (NO<sub>y</sub> ≡ NO<sub>x</sub> + reservoirs). Effective loss of NO<sub>x</sub> from the UT is through subsidence of NO<sub>y</sub> to lower altitudes where deposition of HNO<sub>3</sub> provides the ultimate sink. The residence time of NO<sub>y</sub> in the UT is 10-20 days (Prather and Jacob, 1997). The lifetime of

40 NO<sub>x</sub> against conversion to short-lived reservoirs varies from ~3 hours in the convective outflow of thunderstorms to 0.5-1.5 days  
in background air (Nault et al., 2016). Chemical recycling from these reservoirs maintains relatively high UT NO<sub>x</sub> background  
concentrations (Bradshaw et al., 2000; Baehr et al., 2003; Nault et al., 2016).

45 Representation of lightning NO<sub>x</sub> in chemical transport models (CTMs) is particularly uncertain. Physically-based parameterizations  
relating lightning frequency to deep convective cloud tops, convective mass flux, convective precipitation, or high-cloud ice  
content have poor predictive capability (Tost et al., 2007; Allen et al., 2010; Murray et al., 2012; Finney et al., 2014), limiting our  
ability to estimate the response of lightning NO<sub>x</sub> to future climate (Finney et al., 2016; 2018). An alternative is to prescribe flash  
densities from space-based observations and static NO<sub>x</sub> production rates per flash (Sauvage et al., 2007; Allen et al., 2010; Murray  
et al., 2012). NO<sub>x</sub> production efficiencies per flash in the literature vary from <10 to 5000 moles nitrogen per flash (mol N fl<sup>-1</sup>)  
(Schumann and Huntrieser, 2007; Murray, 2016). Global chemical transport models (CTMs) typically use 100-500 mol N fl<sup>-1</sup>,  
50 sometimes assuming higher production rates at mid-latitudes than in the tropics (Hudman et al., 2007; Ott et al., 2010), and a global  
lightning NO<sub>x</sub> source of 3-7 Tg N a<sup>-1</sup> to match observations of tropospheric ozone and NO<sub>y</sub> species (Sauvage et al., 2007).

Our understanding of UT NO<sub>x</sub> has so far been evaluated with observations from aircraft campaigns (Drummond et al., 1988; Jacob  
et al., 1996; Crawford et al., 1997; Jaeglé et al., 1998; Bradshaw et al., 2000; Hudman et al., 2007; Stratmann et al., 2016). There  
55 are also long-term NO<sub>x</sub> measurements from instruments onboard commercial aircraft dating back to the 1990s, but these are mostly  
over the north Atlantic and the NO<sub>2</sub> measurements have low precision and interference from thermally unstable NO<sub>x</sub> reservoir  
compounds (Brunner et al., 2001). A number of studies have used satellite observations of tropospheric NO<sub>2</sub> columns from solar  
backscatter to infer lightning NO<sub>x</sub> emissions (Beirle et al., 2010; Pickering et al., 2016; [Bucsela et al., 2010](#)), including in  
combination with global models (Boersma et al., 2005; Martin et al., 2007; [Miyazaki et al., 2014](#)). These studies estimate global  
60 lightning NO<sub>x</sub> emission of 1 to 8 Tg N a<sup>-1</sup>.

Deleted: NO<sub>y</sub>

Deleted: ; Bucsela et al., 2010

New cloud-sliced satellite products of tropospheric NO<sub>2</sub> mixing ratios at 280-450 hPa (~6-9 km) offer additional vertical resolution  
by retrieving partial NO<sub>2</sub> columns above clouds and exploiting differences in heights of neighboring clouds to calculate NO<sub>2</sub>  
65 mixing ratios (Choi et al., 2014; Belmonte-Rivas et al., 2015). There are two new products of seasonal mean UT NO<sub>2</sub> mixing ratios  
retrieved from Ozone Monitoring Instrument (OMI) partial NO<sub>2</sub> columns by research groups at KNMI and NASA. The KNMI  
product has been evaluated against UT NO<sub>2</sub> from the Tracer Model version 4 (TM4) CTM. Large regional differences between  
OMI and TM4 are attributed to model deficiencies in lightning NO<sub>x</sub> and uplift of anthropogenic pollution (Belmonte-Rivas et al.,  
2015). The NASA UT product is new to this work and follows a similar retrieval approach to the mid-tropospheric (900-650 hPa)  
product of Choi et al. (2014). That product was evaluated with aircraft observations of NO<sub>2</sub> and interpreted with the Global  
70 Modeling Initiative (GMI) CTM (Choi et al., 2014). Choi et al. (2014) identified large discrepancies between modeled and observed  
NO<sub>2</sub> seasonality over regions influenced by pollution and lightning.

Here we compare the two UT NO<sub>2</sub> products, obtained with distinct retrieval methods, and use aircraft observations of NO<sub>2</sub> from  
multiple NASA DC8 aircraft campaigns to arbitrate and evaluate the information that can be derived from the satellite datasets.  
75 We go on to test current understanding of UT NO<sub>x</sub> and the implications for lightning emissions using the GEOS-Chem CTM.

## 2. OMI observations of upper troposphere NO<sub>2</sub>

80 OMI is onboard the NASA Aura satellite launched into sun-synchronous orbit in July 2004. It has an overpass time of about 13h30 local time (LT), a swath width of 2600 km, and a horizontal resolution of 13 km × 24 km at nadir (Levelt et al., 2006). Columns of NO<sub>2</sub> along the instrument viewing path (slant columns) are obtained by spectral fitting of solar backscattered radiation in the 405-465 nm window (Boersma et al., 2011). Standard products of total and tropospheric column NO<sub>2</sub> are screened for cloudy scenes using a cloud radiance fraction threshold of 0.5. Partial columns of NO<sub>2</sub> above cloudy scenes can be used to estimate vertically resolved NO<sub>2</sub> mixing ratios, as was first demonstrated with satellite observations of ozone (Ziemke et al., 2001). This approach, so-called cloud slicing, assumes a uniform trace gas concentration between two horizontally nearby clouds at different altitudes, so that the UT NO<sub>2</sub> mixing ratio is proportional to the slope of the partial columns versus the corresponding cloud pressures at the optical centre of the cloud. Two products of seasonal mean UT NO<sub>2</sub> have been retrieved from OMI following distinct retrieval steps detailed below: a product from KNMI at 330-450 hPa for 2006 (Belmonte-Rivas et al., 2015) and from NASA at 280-450 hPa for 2005-2007 following an approach similar to that used to retrieve mid-tropospheric NO<sub>2</sub> (Choi et al., 90 2014). In what follows we distinguish the two OMI NO<sub>2</sub> products as KNMI and NASA.

The KNMI product uses DOMINO v2.0 slant columns (Boersma et al., 2011) and OMCLDO2 cloud fractions and altitudes (Acarreta et al., 2004) over partially to very cloudy scenes (cloud radiance fraction > 0.5). Contamination due to NO<sub>2</sub> from below (up to 66% over polluted land masses) is estimated using the TM4 model and removed. Stratospheric NO<sub>2</sub> from an assimilated product (Belmonte-Rivas et al., 2014) is also removed. An air mass factor (AMF) (detailed in Boersma et al. (2004)) that accounts for viewing geometry, surface albedo, light attenuation by gases along the viewing path, and sensitivity to NO<sub>2</sub> vertical distribution is applied to the resultant partial slant columns to convert to vertical columns. Additional data filtering removes scenes with solar zenith angle (SZA) ≥ 70° and surface albedo ≥ 30%. Resultant daily vertical partial columns are aggregated on consistent pressure and horizontal (1° × 1°) grids and used to determine seasonal mean UT NO<sub>2</sub> mixing ratios for gridsquares with at least 30 measurements. UT NO<sub>2</sub> centred at 380 hPa (range 330-450 hPa) is estimated as the difference between partial tropospheric columns retrieved above two neighboring clouds with cloud pressures in the ranges 330-450 hPa and 380-500 hPa, respectively. Biases from sampling cloudy scenes, such as the effect of clouds on photochemistry, are corrected using TM4. These are small (typically <20%) in the UT (Belmonte-Rivas et al., 2015).

105 The NASA UT NO<sub>2</sub> product for 2005-2007, centred at 350 hPa (~280-450 hPa), uses updated version 3 slant columns (OMNO2 v3.0) (Krotkov et al., 2017) that correct for a positive bias in the DOMINO v2.0 product with improved spectral fitting (Marchenko et al., 2015; van Geffen et al., 2015). Partial columns from the cloud height to the top of the atmosphere are retrieved for individual OMI pixels above very cloudy scenes (cloud radiance fraction > 0.7) to minimize contamination from below. Cloud fraction and height is from the OMCLDO2 product (Acarreta et al., 2004). The AMF accounts for viewing path geometry and light scattering by clouds with uniform scatter that are optically thick and geometrically thin (near-Lambertian clouds). Data filtering is applied to remove scenes with SZA > 80°, snow/ice cover, and severe aerosol pollution that could be misclassified as clouds. Daily UT NO<sub>2</sub> is estimated for neighboring partial columns with sufficient cloud variability (cloud pressure distance > 160 hPa) and well-mixed NO<sub>2</sub> (NO<sub>2</sub> vertical gradient < 0.33 pptv hPa<sup>-1</sup> diagnosed with the GMI CTM). The stratospheric column is assumed uniform above neighboring clouds and so is removed when differencing two nearby partial columns. Daily values of UT NO<sub>2</sub> are gridded to obtain seasonal means at 5° × 8° (latitude × longitude) for scenes with at least 50 measurements. Gaussian weighting is applied to assign higher weighting to UT NO<sub>2</sub> closest to 350 hPa. Choi et al. (2014) used a similar approach to retrieve mid-tropospheric NO<sub>2</sub> except that cloud fraction and height were from the OMCLDRR product, and successful retrieval required a stricter cloud radiance fraction of 0.9, a minimum of 30 measurements, and a wider minimum cloud pressure distance of 200 hPa. A shift in cloud radiance fraction

Deleted: and aerosols

Deleted: pressure

Deleted: at 380 hPa to the tropopause and at 380-500 hPa

Deleted: pressure range

Deleted:

Deleted: and,

Deleted: ,

Deleted: ,

Deleted: were used

threshold from 0.9 (Choi et al., 2014) to 0.7 (this work) only introduces a small (<5%) difference in the retrieved partial columns due to contamination from below, as estimated by Pickering et al. (2016) for OMI scenes over the Gulf of Mexico.

130

Figure 1 compares seasonal mean UT NO<sub>2</sub> from the two satellite products in December-February and June-August. KNMI NO<sub>2</sub> is gridded to the NASA coarse grid. Data for March-May and September-November are in the Supplement (Figure S1). KNMI NO<sub>2</sub> has greater coverage than the NASA product, due to a lower cloud fraction threshold in the retrieval. The two products exhibit very different spatial features. Spatial correlation between the two products (Pearson's correlation coefficient between coincident gridsquares) is R = 0.41 in December-February and R = 0.38 in June-August. There is marginal improvement in the correlation with further spatial averaging. At 20° × 32° we find R = 0.50 in December-February and R = 0.45 in June-August. The correlation only increases substantially in September-November from R = 0.49 at 5° × 8° (Figure S1) to R = 0.66 at 20° × 32°. KNMI is systematically lower than NASA in all seasons for coincident gridsquares, varying from 16% lower in June-August to 48% lower in December-February at 20° × 32°.

140

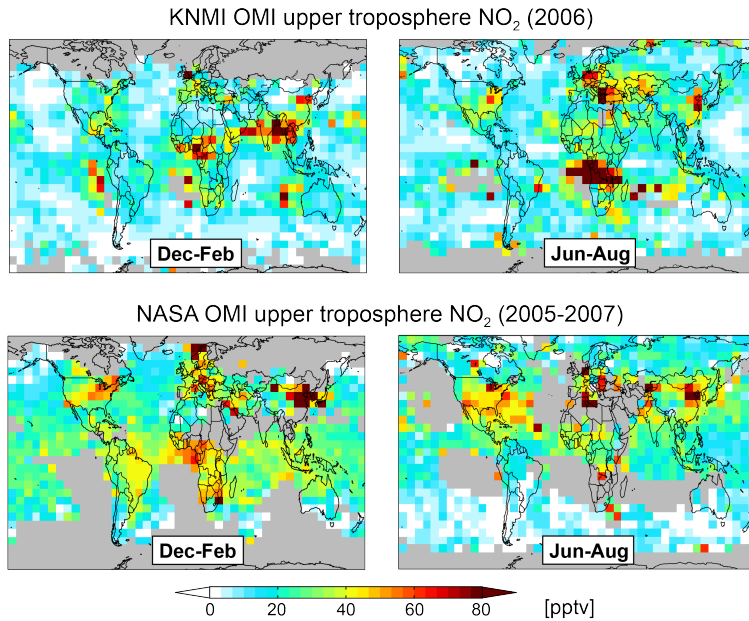


Figure 1. Upper troposphere (UT) NO<sub>2</sub> from the OMI satellite instrument. Seasonal mean UT NO<sub>2</sub> from KNMI in 2006 at 330-450 hPa (top) is compared to NASA in 2005-2007 at 280-450 hPa (bottom). Data are at 5° × 8° horizontal resolution for December-February (left) and June-August (right). Grey areas indicate no data and, for NASA, scenes with fewer than 50 measurements.

145

Contamination of UT NO<sub>2</sub> from below the cloud may still be present in the datasets despite attempts to correct for this using the TM4 model in the case of KNMI and by only considering very cloudy scenes in the case of NASA. These include a large enhancement in KNMI NO<sub>2</sub> (> 90 pptv) over southern Africa in June-August when there is intense biomass burning, and the NO<sub>2</sub> hotspot over northeast China in all seasons in both products (Figures 1, S1). Belmonte-Rivas et al. (2015) caution that the contamination correction in the KNMI product relies on accurate simulation of NO<sub>2</sub> vertical distribution.

150

### 3. Evaluation of OMI upper troposphere NO<sub>2</sub> with aircraft observations

We evaluate the OMI UT NO<sub>2</sub> products with observations from NASA DC8 aircraft campaigns over North America and Greenland in spring-summer, for which dense coverage is available (Figure 2). These include the INTEX-A, INTEX-B, ARCTAS, DC3, and SEAC<sup>4</sup>RS campaigns. Only INTEX-B is in the same year as the OMI products but we consider interannual variability to be only a small source of error. All NO<sub>2</sub> measurements are from thermal-dissociation laser-induced fluorescence (TD-LIF) instruments (Day et al., 2002). These are susceptible to interference from decomposition of thermally unstable reservoir compounds including methyl peroxy nitrate (CH<sub>3</sub>O<sub>2</sub>NO<sub>2</sub>) and HNO<sub>4</sub> (Browne et al., 2011). Publicly available DC3 and SEAC<sup>4</sup>RS TD-LIF NO<sub>2</sub> are already corrected for this interference. We apply a correction for the other campaigns using the relationship between temperature and percentage interference from Browne et al. (2011). Observed mean ambient air temperature in the UT during INTEX-A was 246 K, corresponding to 20% interference. That for INTEX-B was 241 K (30% interference) and 236 K for ARCTAS (38% interference).

There are also NO<sub>2</sub> observations from the recent NASA ATom campaign, and from the In-service Aircraft for a Global Observing System (IAGOS) commercial aircraft campaign (Berkes et al., 2017). These use chemiluminescence instruments that are also susceptible to interference. Chemiluminescence and TD-LIF NO<sub>2</sub> are consistent during the SEAC<sup>4</sup>RS campaign for the altitude range considered in this work (6-9 km) (Travis et al., 2016), but the interference from chemiluminescence is challenging to quantify, due to dependence on the operator and instrument design that varies across campaigns (Reed et al., 2016).

Figure 2 shows the sampling extent of TD-LIF UT NO<sub>2</sub> over North America and Greenland in spring-summer at 450-280 hPa around the satellite overpass (11h00-16h00 LT) for scenes not influenced by the stratosphere (diagnosed with collocated ozone/CO > 1.25 mol mol<sup>-1</sup> (Hudman et al., 2007)). Concentrations of UT NO<sub>2</sub> exceed 80 pptv over the eastern US due to lightning NO<sub>x</sub> emissions and convective transport of boundary layer pollution, and are < 30 pptv over the rest of the domain.

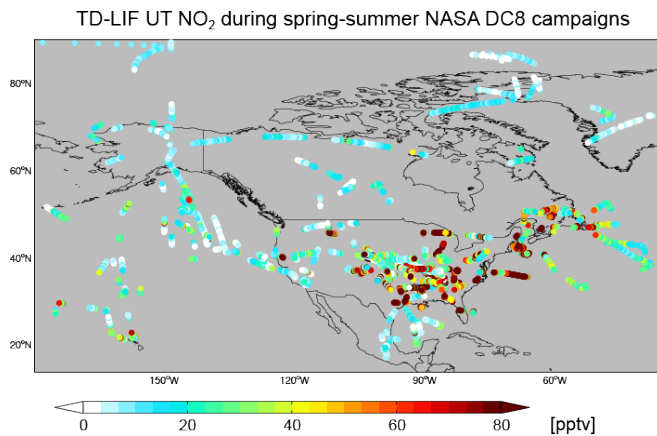


Figure 2. NASA DC8 upper troposphere NO<sub>2</sub> over North America in spring-summer (March-August). Observations are from the TD-LIF instrument at 450-280 hPa, 11h00-16h00 local time, and without stratospheric influence. Campaigns include INTEX-A in June-August 2004 (Singh et al., 2006), INTEX-B in March-May 2006 (Singh et al., 2009), ARCTAS in March-April and June-July 2008 (Jacob et al., 2010), DC3 in May-June 2012 (Barth et al., 2015), and SEAC<sup>4</sup>RS in August 2013 (Toon et al., 2016).

**Deleted:** The aircraft observations we use to

**Deleted:** are from thermal-dissociation laser-induced fluorescence (TD-LIF) instruments (Day et al., 2002) for

**Deleted:** when there is a high density of measurement campaigns

**Deleted:** Measurements of NO<sub>2</sub> from TD-LIF

**Deleted:** , in particular in the UT, where NO<sub>2</sub> concentrations are relatively low, temperature gradients between the instrument inlet and ambient air are large, and reservoir compounds are abundant

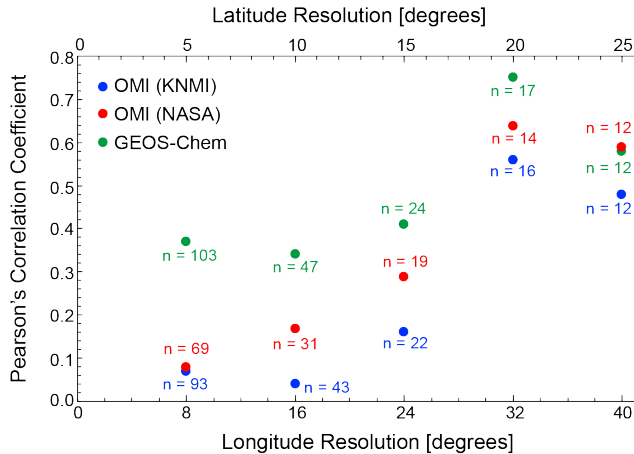
**Deleted:** is

**Deleted:** is

**Deleted:** also



Figure 3 shows the spatial correlation between the March-August mean gridded aircraft data and the OMI UT NO<sub>2</sub> from the KNMI and NASA products as a function of horizontal resolution. There is no significant spatial correlation between the OMI products and aircraft NO<sub>2</sub> at 5° × 8° (R < 0.1) and 10° × 16° (R < 0.2). The correlation improves with further spatial averaging, peaking at 20° × 32° (R = 0.56 for KNMI, R = 0.64 for NASA). The satellite products are also spatially consistent at this resolution (R = 0.89), but KNMI is 43% lower than NASA.



Deleted: 2

Deleted: spatial consistency

Deleted: for both products

Deleted: over this domain

Figure 3. Evaluation of OMI and GEOS-Chem upper troposphere NO<sub>2</sub> with aircraft observations. Individual points are Pearson's correlation coefficients between gridded March-August mean UT NO<sub>2</sub> measured from the aircraft and OMI KNMI in 2006 (blue), OMI NASA in 2005-2007 (red), and GEOS-Chem in 2006 (green), for grid averaging domains of 5° × 8° (latitude × longitude), 10° × 16°, 15° × 24°, 20° × 32°, and 25° × 40°. Values inset are the number of points at each resolution. The domain sampled is shown in Figure 2.

Deleted: at

Figure 4 compares the spatial distribution of OMI and aircraft UT NO<sub>2</sub> at 20° × 32° over North America. Domain mean KNMI UT NO<sub>2</sub> is 38% lower than the aircraft observations, compared to 2.2% higher for NASA UT NO<sub>2</sub>. Both products exhibit less variability (reduced major axis, RMA, regression slopes < 1) and high bias in background NO<sub>2</sub> compared to the aircraft observations (positive RMA intercepts of 5.9 ± 1.4 pptv for KNMI and 9.2 ± 2.7 pptv for NASA). We proceed with the NASA UT NO<sub>2</sub> product at 20° × 32°, as correlation peaks at this resolution and the NASA product is more consistent with domain mean aircraft UT NO<sub>2</sub> than the KNMI product.

#### 4. Constraints on upper tropospheric NO<sub>x</sub>

The NASA product provides near-global coverage of UT NO<sub>2</sub> to assess current understanding of regional UT NO<sub>x</sub> sources and dynamics by comparing to UT NO<sub>2</sub> from the GEOS-Chem CTM (version 10-01; [http://wiki.seas.harvard.edu/geos-chem/index.php/GEOS-Chem\\_v10-01](http://wiki.seas.harvard.edu/geos-chem/index.php/GEOS-Chem_v10-01)) driven with NASA MERRA-2 reanalysis meteorology. The model horizontal resolution is 2° × 2.5° and the output is regridded to 20° × 32° for comparison with OMI. GEOS-Chem is sampled under all-sky conditions in the satellite overpass window (12h00-15h00 local time). We find that the effect on NO<sub>2</sub> of sampling the model under cloudy conditions is small. Isolating NO<sub>2</sub> under very cloudy conditions using MERRA-2 cloud fractions decreases modeled UT NO<sub>2</sub> by no more than 5 pptv in the tropics/subtropics and less at higher latitudes. We use output from the model for 2006 following a one-

year spin-up for chemical initialization. Interannual variability in UT NO<sub>2</sub>, determined as the difference between modeled 2006 and multi-year mean (2005-2007) UT NO<sub>2</sub>, is small (< 4 pptv) everywhere except central Africa year-round (4-12 pptv), the Arctic north of 60°N (up to 25 pptv), and the Middle East in June-August and northern India in March-May (both 10-20 pptv). Recent evaluation of model NO<sub>2</sub> with observed vertical profiles from the SEAC<sup>4</sup>RS aircraft campaign show no significant bias in the 6-9 km range of the OMI product (Travis et al., 2016; Silvern et al., 2018).

Deleted: (

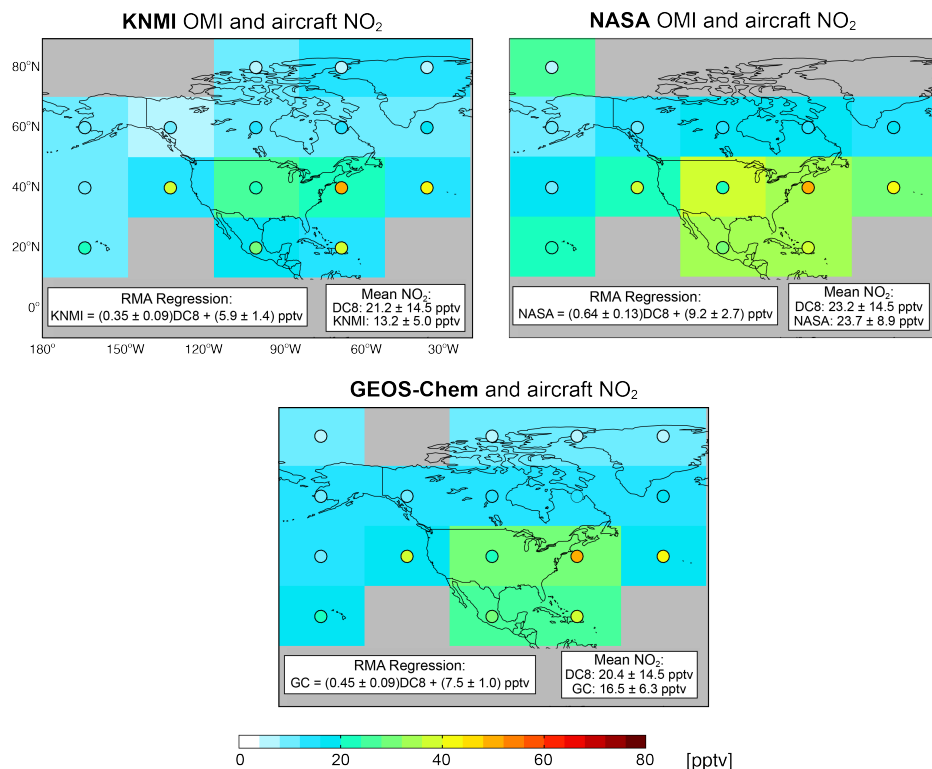


Figure 4. March-August upper troposphere NO<sub>2</sub> over North America. All data are at 20° × 32°. Background colors in the different panels show concentrations from KNMI, NASA, and GEOS-Chem (GC). Circles show the aircraft observations (same in all panels). Aircraft observations are for 11h00-16h00 local time (LT). The model is sampled in the satellite overpass time window (12h00-15h00 LT). Model and aircraft data are at 280-450 hPa and screened for stratospheric influence using ozone/CO > 1.25 mol mol<sup>-1</sup>. Inset boxes show reduced major axis (RMA) regression statistics and mean NO<sub>2</sub> for coincident gridsquares. Grey gridsquares indicate no observations.

Local GEOS-Chem emissions of NO<sub>x</sub> in the UT include aircraft and lightning. Aircraft emissions from the AEIC inventory (Stettler et al., 2011) total 0.82 Tg N in 2006; much less than lightning in the same year (6.5 Tg N). Transport from the stratosphere is simulated using a climatology of NO<sub>x</sub> species concentrations from the GMI model above the tropopause (Murray et al., 2012) and is very small (0.4 Tg N a<sup>-1</sup> as total NO<sub>x</sub>). Lightning in the model is estimated using the parameterization implemented by Murray et al. (2012). This includes an initial estimate of lightning flashes using the Price and Rind (1992, 1993, 1994) relationship between cloud-top height and lightning flashes. These are then scaled to the same annual global flash frequency (46 fl s<sup>-1</sup>) and regional

distribution as the climatology from the combined Lightning Imaging Sensor (LIS) and Optical Transient Detector (OTD) high-resolution monthly climatology (LIS/OTD HRMC) (Cecil et al., 2014). The standard GEOS-Chem model has higher NO<sub>x</sub> yields per flash at northern mid-latitudes (north of 35°N) than in the tropics (500 mol N fl<sup>-1</sup> versus 260 mol N fl<sup>-1</sup>), but we find that this overestimates observed OMI UT NO<sub>2</sub> by 10-20 pptv (20-40%) at northern mid-latitudes in summer when the lightning source is dominant. Here we address this overestimate by assuming a NO<sub>x</sub> yield of 260 mol N fl<sup>-1</sup> everywhere. This decreases global lightning NO<sub>x</sub> emissions by 15% from 6.5 to 5.5 Tg N a<sup>-1</sup>. The lightning parameterization in GEOS-Chem does not distinguish lightning NO<sub>x</sub> production from flashes within or between clouds (intra- or inter-cloud) or from the cloud to the Earth's surface (cloud-to-ground).

Figure 3 shows the spatial correlation between the model and aircraft observations. The model is more consistent with the aircraft observations than OMI at fine spatial resolution. Like OMI, GEOS-Chem correlation with the aircraft observations improves with spatial averaging, peaking at 20° × 32° (R = 0.75). Figure 4 also shows comparison of March-August GEOS-Chem UT NO<sub>2</sub> with the aircraft observations at 20° × 32°. The model is sampled over the same pressure range as NASA (280-450 hPa) around the OMI overpass (12h00-15h00 LT) and is filtered for stratospheric influence using model ozone/CO > 1.25 mol mol<sup>-1</sup>. Domain average UT NO<sub>2</sub> from the model is 19% lower than the aircraft measurements and the model also overestimates background UT NO<sub>2</sub> (intercept = 7.5 ± 1.0 pptv) and underestimates the variability (slope = 0.45 ± 0.09).

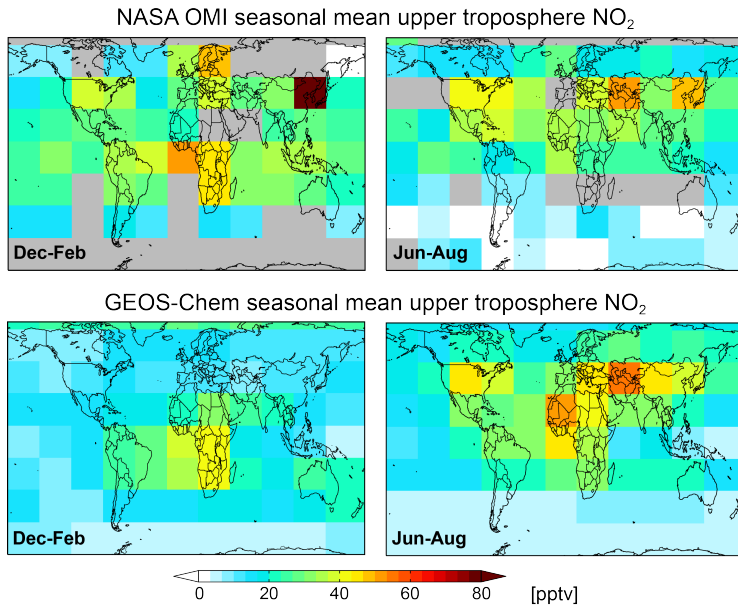
Figure 5 compares seasonal mean OMI and GEOS-Chem UT NO<sub>2</sub> in December-February and June-August. The other seasons are shown in the Supplement (Figure S2). Formation of PAN, HNO<sub>4</sub> and CH<sub>3</sub>O<sub>2</sub>NO<sub>2</sub> accounts for over 75% of NO<sub>x</sub> loss in the model in all seasons. Lower concentrations of UT NO<sub>2</sub> in the northern hemisphere winter compared to summer in the model is mostly because lightning activity is at a minimum. The model underestimates UT NO<sub>2</sub> in the northern mid-latitudes in winter by 20-40 pptv, suggesting misrepresentation of another process in the model, such as excessive NO<sub>x</sub> loss by N<sub>2</sub>O<sub>5</sub> hydrolysis in aerosols (Kenagy et al., 2018). The particularly large bias over polluted regions in winter could also be due to contamination of the UT NO<sub>2</sub> retrievals by enhanced boundary layer NO<sub>2</sub>.

Deleted: d

Deleted: for

Deleted: and

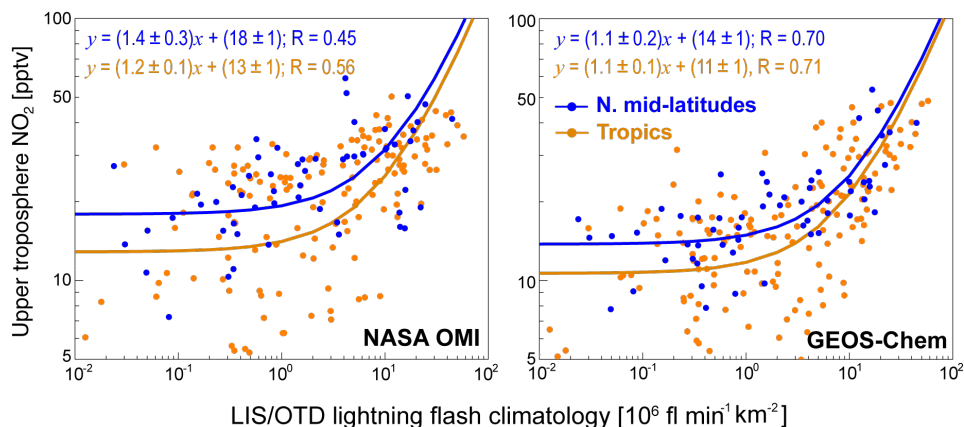
Deleted: and



275 **Figure 5. Observed and modelled upper troposphere NO<sub>2</sub>. The figure shows NASA OMI seasonal mean UT NO<sub>2</sub> for 2005-2007 (top) and corresponding GEOS-Chem model values (bottom). The model is sampled at 280-450 hPa during the satellite overpass (12h00-15h00 LT), and filtered for stratospheric influence. Data are at 20° × 32° horizontal resolution for December-February (left) and June-August (right). Grey gridsquares in the top panel indicate no OMI data.**

280 Figure 6 shows the log-log relationship between seasonal mean LIS/OTD lightning flash climatology and seasonal mean UT NO<sub>2</sub> from OMI and GEOS-Chem, and the corresponding reduced major axis linear regression fits. Data are divided into northern mid-latitudes and tropics. We exclude the contaminated observations over northeast China and the wintertime northern mid-latitude gridsquares that show no correlation with lightning flashes (R < 0.1). Results from multi-model sensitivity studies indicate that UT NO<sub>x</sub> in winter is predominantly from surface sources, with a smaller contribution from extra-tropical lightning (Grewe et al., 2001). Background concentration of UT NO<sub>2</sub> (intercepts in Figure 6) from non-lightning sources is 10-20 pptv and is 3-5 pptv higher in the northern mid-latitudes than the tropics. The slopes for the linear fits to lightning flash frequency are consistent between the OMI observations and GEOS-Chem, and show similar slopes for northern mid-latitudes and the tropics. Fitting the ratio between OMI observations and GEOS-Chem on the 20° × 32° grid implies a NO<sub>x</sub> yield per flash of 280 ± 80 mol N fl<sup>-1</sup> with no significant difference between mid-latitudes and the tropics, and no significant difference with the GEOS-Chem prior estimate of 260 mol N fl<sup>-1</sup>. Our prior estimate of global lightning source was 5.5 Tg N a<sup>-1</sup>, and the improved estimate is 5.9 ± 1.7 Tg N a<sup>-1</sup>.

- Deleted: linear
- Deleted:
- Deleted: seasonal means and
- Deleted: ,
- Deleted: to the observations and model are similar for the
- Formatted: Subscript
- Formatted: Superscript
- Formatted: Superscript
- Formatted: Superscript
- Formatted: Superscript
- Deleted: , providing no support for the previously reported higher lightning NO<sub>x</sub> production rates in the mid-latitudes than the tropics.



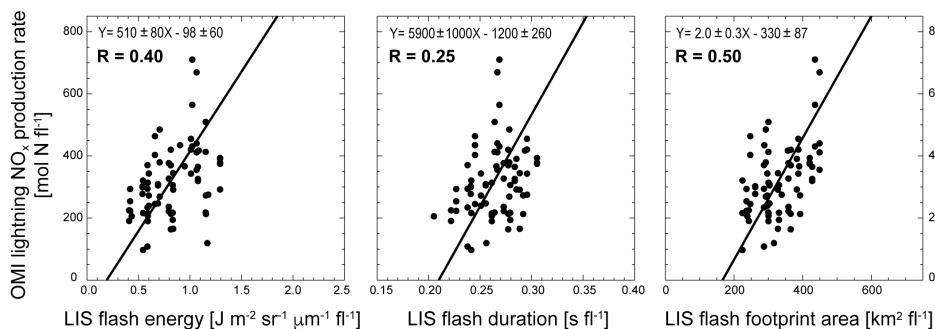
300 **Figure 6. Log-log relationship between upper troposphere NO<sub>2</sub> and lightning flash frequencies, and linear regression fits between the two.** Individual points are coincident seasonal mean UT NO<sub>2</sub> from OMI (left) and GEOS-Chem (right) versus seasonal mean LIS/OTD lightning flash climatologies for coincident 20° × 32° gridsquares in the northern mid-latitudes (> 30°N; blue) and tropics (< 30°N; orange). Northern mid-latitude points exclude December-February that show poor correlation with lightning flashes (see text for details). Lines and legends show reduced major axis linear regression fits to the data with corresponding Pearson's correlation coefficients. The regression lines plot as curves on the log-log scale, highlighting the NO<sub>2</sub> background at low lightning flash rates and the correlation of NO<sub>2</sub> with lightning at high flash rates.

Deleted: Linear

Deleted: plotted on logarithmic scales. Values inset are

Deleted: and RMA regression statistics

Deleted: We go on to obtain OMI-constrained lightning NO<sub>x</sub> production rates by scaling 260 mol N fl<sup>-1</sup> by the ratio of OMI to GEOS-Chem UT NO<sub>2</sub> estimated in each 20° × 32° gridsquare (local discrepancies between the observations and model). Resultant local OMI and GEOS-Chem-derived production rates vary from 100 to 900 mol N fl<sup>-1</sup> and values are higher in the tropics (300 ± 60 mol N fl<sup>-1</sup>) than the northern mid-latitudes (270 ± 100 mol N fl<sup>-1</sup>), but the difference is not significant. The global average (280 ± 80 mol N fl<sup>-1</sup>) is similar to 310 mol N fl<sup>-1</sup> obtained by assimilating multiple satellite observations of atmospheric composition (Miyazaki et al., 2014).<sup>4</sup>



310 **Figure 7. Relationship between OMI and GEOS-Chem derived lightning NO<sub>x</sub> production rates and LIS lightning properties: energy (radiance), duration, and footprint area.** Individual points are seasonal mean 20° × 32° gridsquares at 40°N-40°S.

315 Properties of lightning flashes including energy, duration, and footprint area, have been retrieved from the OTD and LIS sensors (Beirle et al., 2014). The flash footprint area is the spatial extent of lightning detection events contributing to the flash (collection of local events) diagnosed by the satellite data. Figure 7 shows the relationship between OMI and GEOS-Chem derived lightning NO<sub>x</sub> production rates and LIS lightning properties from Beirle et al. (2014). The strongest correlation is with lightning extent (R = 0.50), followed by energy (R = 0.40). The correlation with flash duration is weak (R = 0.25). The relationships in Figure 7 suggest a dependence of lightning NO<sub>x</sub> production rates on lightning flash energy of 510 ± 80 mol N (J m<sup>-2</sup> sr<sup>-1</sup> μm<sup>-1</sup>)<sup>-1</sup> and on flash footprint

area of  $2.0 \pm 0.3 \text{ mol N km}^{-2}$ , possibly offering guidance for relating  $\text{NO}_x$  yields to physical properties in global models rather than the current approach of assigning static values.

## 5. Conclusions

Measurements of  $\text{NO}_x$  in the upper troposphere (UT) have mainly been from aircraft campaigns that are limited in space and time. Two new cloud-slicing UT  $\text{NO}_2$  products from the Ozone Monitoring Instrument (OMI) produced by KNMI and NASA offer the potential to address uncertainties in our understanding of UT  $\text{NO}_x$  sources. Here we intercompared these products, evaluated them with aircraft observations, and used them together with GEOS-Chem model simulations to demonstrate a dominance of lightning as a source of UT  $\text{NO}_x$ .

The KNMI and NASA UT  $\text{NO}_2$  products use very different retrieval methods. Seasonal mean concentrations from the two products show weak global correlation at the  $5^\circ \times 8^\circ$  (latitude  $\times$  longitude) resolution of the NASA retrieval, with some improvement when the data are further averaged to  $20^\circ \times 32^\circ$  ( $R = 0.5\text{-}0.7$ ). At that resolution they show correlation with in situ aircraft observations of UT  $\text{NO}_2$  over North America for different years ( $R = 0.56\text{-}0.64$ ). The KNMI product is biased low by 38% relative to the aircraft observations while the NASA product has no significant bias.

We find from the relationship of OMI UT  $\text{NO}_2$  with LIS/OTD flash rates that most  $\text{NO}_x$  in the upper troposphere is from lightning, except in the mid-latitudes in winter. The background  $\text{NO}_2$  concentration in the absence of lightning is 10-20 pptv. The relationship suggests no difference in  $\text{NO}_x$  yields per flash between the mid-latitudes and the tropics, in contrast to the higher yields at mid-latitudes often assumed in models. We derive a global mean lightning  $\text{NO}_x$  production rate per flash of  $280 \pm 80 \text{ mol N fl}^{-1}$ , from which we infer a best estimate for the global lightning  $\text{NO}_x$  emission of  $5.9 \pm 1.7 \text{ Tg N a}^{-1}$ .

## Data Availability

Data from this work can be made available upon request: E. A. Marais for GEOS-Chem output, M. Belmonte-Rivas for KNMI OMI UT  $\text{NO}_2$ , S. Choi and J. Joiner for NASA OMI UT  $\text{NO}_2$ , and S. Beirle for LIS lightning properties.

## Competing Interests

The authors declare that they have no conflicts of interest.

## Author Contributions

EAM conducted model simulations, analysed and interpreted satellite, model, and aircraft data, and prepared the manuscript, DJJ provided supervisory guidance and assisted in the writing. SC, JJ, and MR-B retrieved the OMI UT  $\text{NO}_2$  products, RCC aided in interpreting aircraft observations., LTM contributed LIS/OTD lightning flash observations, SB contributed lightning flash properties, LS, VS, and LJ contributed updated GEOS-Chem code.

## Acknowledgements

Deleted: The majority of m

Deleted: are

Deleted: measurement

Deleted: W

Deleted: to

Deleted: test and improve the

Deleted: representation of UT  $\text{NO}_x$

Deleted: They have

Deleted: ,  $R = 0.4$ , and only marginal

Deleted: extended

Deleted: The OMI data only provide coarse information on UT  $\text{NO}_2$ , but measurements from the recently launched TROPOMI instrument with  $7 \text{ km} \times 3.5 \text{ km}$  nadir pixel resolution (compared to  $13 \text{ km} \times 24 \text{ km}$  for OMI) may be able to provide finer information in the future.

Deleted: that

Deleted: suggests

Deleted: also

Deleted: and

Deleted: s

Deleted: 5

This work was funded by the NASA Tropospheric Chemistry Program and a University of Birmingham Research Fellowship and NERC/EPSC grant (EP/R513465/1) awarded to E. A. Marais. Model simulations were performed on the University of Birmingham's BlueBEAR High Performance Cluster. The authors would like to thank the BlueBEAR support team for IT and HPC support.

## 390 References

- Acarreta, J. R., De Haan, J. F., and Stammes, P.: Cloud pressure retrieval using the O<sub>2</sub>-O<sub>2</sub> absorption band at 477 nm, *J. Geophys. Res.*, 109, doi:10.1029/2003jd003915, 2004.
- Allen, D., Pickering, K., Duncan, B., and Damon, M.: Impact of lightning NO emissions on North American photochemistry as determined using the Global Modeling Initiative (GMI) model, *J. Geophys. Res.*, 115, doi:10.1029/2010jd014062, 2010.
- 395 Baehr, J., Schlager, H., Ziereis, H., Stock, P., van Velthoven, P., Busen, R., Strom, J., and Schumann, U.: Aircraft observations of NO, NO<sub>2</sub>, CO, and O<sub>3</sub> in the upper troposphere from 60°N to 60°S - Interhemispheric differences at midlatitudes, *Geophys. Res. Lett.*, 30, doi:10.1029/2003gl016935, 2003.
- Barth, M. C., Cantrell, C. A., Brune, W. H., Rutledge, S. A., Crawford, J. H., Huntrieser, H., Carey, L. D., MacGorman, D., Weisman, M., Pickering, K. E., Bruning, E., Anderson, B., Apel, E., Biggerstaff, M., Campos, T., Campuzano-Jost, P., Cohen, R., Crouse, J., Day, D. A., Diskin, G., Flocke, F., Fried, A., Garland, C., Heikes, B., Honomichl, S., Hornbrook, R., Huey, L. G., Jimenez, J. L., Lang, T., Lichtenstern, M., Mikoviny, T., Nault, B., O'Sullivan, D., Pan, L. L., Peischl, J., Pollack, I., Richter, D., Riemer, D., Ryerson, T., Schlager, H., St Clair, J., Walega, J., Weibring, P., Weinheimer, A., Wennberg, P., Wisthaler, A., Wooldridge, P. J., and Ziegler, C.: The Deep Convective Clouds and Chemistry (DC3) Field Campaign, *B. Am. Meteorol. Soc.*, 96, 1281-1309, doi:10.1175/Bams-D-13-00290.1, 2015.
- 400 Beirle, S., Huntrieser, H., and Wagner, T.: Direct satellite observation of lightning-produced NO<sub>x</sub>, *Atmos. Chem. Phys.*, 10, 10965-10986, doi:10.5194/acp-10-10965-2010, 2010.
- Beirle, S., Koshak, W., Blakeslee, R., and Wagner, T.: Global patterns of lightning properties derived by OTD and LIS, *Nat Hazard Earth Sys*, 14, 2715-2726, doi:10.5194/nhess-14-2715-2014, 2014.
- Belmonte-Rivas, M. B., Veeffkind, P., Boersma, F., Levelt, P., Eskes, H., and Gille, J.: Intercomparison of daytime stratospheric NO<sub>2</sub> satellite retrievals and model simulations, *Atmos. Meas. Tech.*, 7, 2203-2225, doi:10.5194/amt-7-2203-2014, 2014.
- 410 Belmonte-Rivas, M. B., Veeffkind, P., Eskes, H., and Levelt, P.: OMI tropospheric NO<sub>2</sub> profiles from cloud slicing: constraints on surface emissions, convective transport and lightning NO<sub>x</sub>, *Atmos. Chem. Phys.*, 15, 13519-13553, doi:10.5194/acp-15-13519-2015, 2015.
- Berkes, F., Houben, N., Bundke, U., Franke, H., Pätz, H.-W., Rohrer, F., Wahner, A., and Petzold, A.: The IAGOS NO<sub>x</sub> Instrument – Design, operation and first results from deployment aboard passenger aircraft, *Atmos. Meas. Tech.*, doi:10.5194/amt-2017-435, 2017.
- 415 Bertram, T. H., Perring, A. E., Wooldridge, P. J., Crouse, J. D., Kwan, A. J., Wennberg, P. O., Scheuer, E., Dibb, J., Avery, M., Sachse, G., Vay, S. A., Crawford, J. H., McNaughton, C. S., Clarke, A., Pickering, K. E., Fuelberg, H., Huey, G., Blake, D. R., Singh, H. B., Hall, S. R., Shetter, R. E., Fried, A., Heikes, B. G., and Cohen, R. C.: Direct measurements of the convective recycling of the upper troposphere, *Science*, 315, 816-820, doi:10.1126/science.1134548, 2007.
- 420 Boersma, K. F., Eskes, H. J., and Brinksma, E. J.: Error analysis for tropospheric NO<sub>2</sub> retrieval from space, *J. Geophys. Res.*, 109, doi:10.1029/2003jd003962, 2004.
- Boersma, K. F., Eskes, H. J., Meijer, E. W., and Kelder, H. M.: Estimates of lightning NO<sub>x</sub> production from GOME satellite observations, *Atmos. Chem. Phys.*, 5, 2311-2331, doi:10.5194/acp-5-2311-2005, 2005.
- 425 Boersma, K. F., Eskes, H. J., Dirksen, R. J., van der A, R. J., Veeffkind, J. P., Stammes, P., Huijnen, V., Kleipool, Q. L., Sneep, M., Claas, J., Leitao, J., Richter, A., Zhou, Y., and Brunner, D.: An improved tropospheric NO<sub>2</sub> column retrieval algorithm for the Ozone Monitoring Instrument, *Atmos. Meas. Tech.*, 4, 1905-1928, doi:10.5194/amt-4-1905-2011, 2011.
- Bradshaw, J., Davis, D., Grodzinsky, G., Smyth, S., Newell, R., Sandholm, S., and Liu, S.: Observed distributions of nitrogen oxides in the remote free troposphere from the NASA global tropospheric experiment programs, *Rev. Geophys.*, 38, 61-116, doi:10.1029/1999rg900015, 2000.
- 430 Browne, E. C., Perring, A. E., Wooldridge, P. J., Apel, E., Hall, S. R., Huey, L. G., Mao, J., Spencer, K. M., St Clair, J. M., Weinheimer, A. J., Wisthaler, A., and Cohen, R. C.: Global and regional effects of the photochemistry of CH<sub>3</sub>O<sub>2</sub>NO<sub>2</sub>: evidence from ARCTAS, *Atmos. Chem. Phys.*, 11, 4209-4219, doi:10.5194/acp-11-4209-2011, 2011.
- 435 Brunner, D., Staehelin, J., Jeker, D., Wernli, H., and Schumann, U.: Nitrogen oxides and ozone in the tropopause region of the Northern Hemisphere: Measurements from commercial aircraft in 1995/1996 and 1997, *J. Geophys. Res.*, 106, 27673-27699, doi:10.1029/2001jd900239, 2001.

- Bucsela, E. J., Pickering, K. E., Huntemann, T. L., Cohen, R. C., Perring, A., Gleason, J. F., Blakeslee, R. J., Albrecht, R. I., Holzworth, R., Cipriani, J. P., Vargas-Navarro, D., Mora-Segura, I., Pacheco-Hernandez, A., and Laporte-Molina, S.: Lightning-generated NO<sub>x</sub> seen by the Ozone Monitoring Instrument during NASA's Tropical Composition, Cloud and Climate Coupling Experiment (TC4), *J. Geophys. Res.*, 115, doi:10.1029/2009jd013118, 2010.
- 440 Cecil, D. J., Buechler, D. E., and Blakeslee, R. J.: Gridded lightning climatology from TRMM-LIS and OTD: Dataset description, *Atmos. Res.*, 135, 404-414, doi:10.1016/j.atmosres.2012.06.028, 2014.
- Choi, S., Joiner, J., Choi, Y., Duncan, B. N., Vasilkov, A., Krotkov, N., and Bucsela, E.: First estimates of global free-tropospheric NO<sub>2</sub> abundances derived using a cloud-slicing technique applied to satellite observations from the Aura Ozone Monitoring Instrument (OMI), *Atmos. Chem. Phys.*, 14, 10565-10588, doi:10.5194/acp-14-10565-2014, 2014.
- 445 Crawford, J. H., Davis, D. D., Chen, G., Bradshaw, J., Sandholm, S., Kondo, Y., Merrill, J., Liu, S., Browell, E., Gregory, G., Anderson, B., Sachse, G., Barrick, J., Blake, D., Talbot, R., and Poeschel, R.: Implications of large scale shifts in tropospheric NO<sub>x</sub> levels in the remote tropical Pacific, *J. Geophys. Res.*, 102, 28447-28468, doi:10.1029/97jd00011, 1997.
- Dahlmann, K., Grewe, V., Ponater, M., and Matthes, S.: Quantifying the contributions of individual NO<sub>x</sub> sources to the trend in ozone radiative forcing, *Atmos. Environ.*, 45, 2860-2868, doi:10.1016/j.atmosenv.2011.02.071, 2011.
- 450 Day, D. A., Wooldridge, P. J., Dillon, M. B., Thornton, J. A., and Cohen, R. C.: A thermal dissociation laser-induced fluorescence instrument for in situ detection of NO<sub>2</sub>, peroxy nitrates, alkyl nitrates, and HNO<sub>3</sub>, *J. Geophys. Res.*, 107, doi:10.1029/2001jd000779, 2002.
- Drummond, J. W., Ehhalt, D. H., and Volz, A.: Measurements of nitric oxide between 0-12 km altitude and 67°N to 60°S latitude obtained during STRATOZ III, *J. Geophys. Res.*, 93, 15831-15849, doi:10.1029/JD093iD12p15831, 1988.
- 455 Ehhalt, D. H., Rohrer, F., and Wahner, A.: Sources and distribution of NO<sub>x</sub> in the upper troposphere at northern midlatitudes, *J. Geophys. Res.*, 97, 3725-3738, doi:10.1029/91JD03081, 1992.
- Finney, D. L., Doherty, R. M., Wild, O., Huntrieser, H., Pumphrey, H. C., and Blyth, A. M.: Using cloud ice flux to parametrise large-scale lightning, *Atmos. Chem. Phys.*, 14, 12665-12682, doi:10.5194/acp-14-12665-2014, 2014.
- 460 Finney, D. L., Doherty, R. M., Wild, O., Young, P. J., and Butler, A.: Response of lightning NO<sub>x</sub> emissions and ozone production to climate change: Insights from the Atmospheric Chemistry and Climate Model Intercomparison Project, *Geophys. Res. Lett.*, 43, 5492-5500, doi:10.1002/2016gl068825, 2016.
- Finney, D. L., Doherty, R. M., Wild, O., Stevenson, D. S., MacKenzie, I. A., and Blyth, A. M.: A projected decrease in lightning under climate change, *Nat. Clim. Change*, 8, 210-213, doi:10.1038/s41558-018-0072-6, 2018.
- 465 Grewe, V., Brunner, D., Dameris, M., Grenfell, J. L., Hein, R., Shindell, D., and Staehelin, J.: Origin and variability of upper tropospheric nitrogen oxides and ozone at northern mid-latitudes, *Atmos. Environ.*, 35, 3421-3433, doi:10.1016/S1352-2310(01)00134-0, 2001.
- Hudman, R. C., Jacob, D. J., Turquety, S., Leibensperger, E. M., Murray, L. T., Wu, S., Gilliland, A. B., Avery, M., Bertram, T. H., Brune, W., Cohen, R. C., Dibb, J. E., Flocke, F. M., Fried, A., Holloway, J., Neuman, J. A., Orville, R., Perring, A., Ren, X., Sachse, G. W., Singh, H. B., Swanson, A., and Wooldridge, P. J.: Surface and lightning sources of nitrogen oxides over the United States: Magnitudes, chemical evolution, and outflow, *J. Geophys. Res.*, 112, doi:10.1029/2006jd007912, 2007.
- 470 Jacob, D. J., Heikes, B. G., Fan, S. M., Logan, J. A., Mauzerall, D. L., Bradshaw, J. D., Singh, H. B., Gregory, G. L., Talbot, R. W., Blake, D. R., and Sachse, G. W.: Origin of ozone and NO<sub>x</sub> in the tropical troposphere: A photochemical analysis of aircraft observations over the South Atlantic basin, *J. Geophys. Res.*, 101, 24235-24250, doi:10.1029/96jd00336, 1996.
- 475 Jacob, D. J., Crawford, J. H., Maring, H., Clarke, A. D., Dibb, J. E., Emmons, L. K., Ferrare, R. A., Hostetler, C. A., Russell, P. B., Singh, H. B., Thompson, A. M., Shaw, G. E., McCauley, E., Pederson, J. R., and Fisher, J. A.: The Arctic Research of the Composition of the Troposphere from Aircraft and Satellites (ARCTAS) mission: design, execution, and first results, *Atmos. Chem. Phys.*, 10, 5191-5212, doi:10.5194/acp-10-5191-2010, 2010.
- 480 Jaeglé, L., Jacob, D. J., Wang, Y., Weinheimer, A. J., Ridley, B. A., Campos, T. L., Sachse, G. W., and Hagen, D. E.: Sources and chemistry of NO<sub>x</sub> in the upper troposphere over the United States, *Geophys. Res. Lett.*, 25, 1705-1708, doi:10.1029/97gl03591, 1998.
- Kenagy, H. S., Sparks, T. L., Ebben, C. J., Wooldridge, P. J., Lopez-Hilfiker, F., Lee, B. H., Thornton, J. A., McDuffe, E. E., Fibiger, D. L., Brown, S. S., Montzka, D. D., Weinheimer, A. J., Schroder, J. C., Campuzano-Jost, P., Day, D. A., Jimenez, J. L., Dibb, J. E., Campos, T., Shah, V., Jaeglé, L., and Cohen, R. C.: NO<sub>x</sub> Lifetime and NO<sub>y</sub> Partitioning During WINTER, *J. Geophys. Res.*, 123, doi:10.1029/2018JD028736, 2018.
- 485 Krotkov, N. A., Lamsal, L. N., Celarier, E. A., Swartz, W. H., Marchenko, S. V., Bucsela, E. J., Chan, K. L., Wenig, M., and Zara, M.: The version 3 OMI NO<sub>2</sub> standard product, *Atmos. Meas. Tech.*, 10, 3133-3149, doi:10.5194/amt-10-3133-2017, 2017.
- 490 Levelt, P. F., Van den Oord, G. H. J., Dobber, M. R., Malkki, A., Visser, H., de Vries, J., Stammes, P., Lundell, J. O. V., and Saari, H.: The Ozone Monitoring Instrument, *IEEE T. Geosci. Remote*, 44, 1093-1101, doi:10.1109/Tgrs.2006.872333, 2006.



- Marchenko, S., Krotkov, N. A., Lamsal, L. N., Celarier, E. A., Swartz, W. H., and Bucseła, E. J.: Revising the slant column density retrieval of nitrogen dioxide observed by the Ozone Monitoring Instrument, *J. Geophys. Res.*, 120, 5670-5692, doi:10.1002/2014jd022913, 2015.
- 495 Martin, R. V., Sauvage, B., Folkins, I., Sioris, C. E., Boone, C., Bernath, P., and Ziemke, J.: Space-based constraints on the production of nitric oxide by lightning, *J. Geophys. Res.*, 112, doi:10.1029/2006jd007831, 2007.
- Miyazaki, K., Eskes, H. J., Sudo, K., and Zhang, C.: Global lightning NO<sub>x</sub> production estimated by an assimilation of multiple satellite data sets, *Atmos. Chem. Phys.*, 14, 3277-3305, doi:10.5194/acp-14-3277-2014, 2014.
- 500 Murray, L. T., Jacob, D. J., Logan, J. A., Hudman, R. C., and Koshak, W. J.: Optimized regional and interannual variability of lightning in a global chemical transport model constrained by LIS/OTD satellite data, *J. Geophys. Res.*, 117, doi:10.1029/2012jd017934, 2012.
- Murray, L. T., Mickley, L. J., Kaplan, J. O., Sofen, E. D., Pfeiffer, M., and Alexander, B.: Factors controlling variability in the oxidative capacity of the troposphere since the Last Glacial Maximum, *Atmos. Chem. Phys.*, 14, 3589-3622, doi:10.5194/acp-14-3589-2014, 2014.
- 505 Murray, L. T.: Lightning NO<sub>x</sub> and Impacts on Air Quality, *Current Pollution Reports*, 2, 115-133, doi:10.1007/s40726-016-0031-7, 2016.
- Nault, B. A., Garland, C., Wooldridge, P. J., Brune, W. H., Campuzano-Jost, P., Crouse, J. D., Day, D. A., Dibb, J., Hall, S. R., Huey, L. G., Jimenez, J. L., Liu, X. X., Mao, J. Q., Mikoviny, T., Peischl, J., Pollack, I. B., Ren, X. R., Ryerson, T. B., Scheuer, E., Ullmann, K., Wennberg, P. O., Wisthaler, A., Zhang, L., and Cohen, R. C.: Observational Constraints on the Oxidation of NO<sub>x</sub> in the Upper Troposphere, *J. Phys. Chem. A*, 120, 1468-1478, doi:10.1021/acs.jpca.5b07824, 2016.
- 510 Ott, L. E., Pickering, K. E., Stenichkov, G. L., Allen, D. J., DeCaria, A. J., Ridley, B., Lin, R. F., Lang, S., and Tao, W. K.: Production of lightning NO<sub>x</sub> and its vertical distribution calculated from three-dimensional cloud-scale chemical transport model simulations, *J. Geophys. Res.*, 115, doi:10.1029/2009jd011880, 2010.
- 515 Pickering, K. E., Bucseła, E., Allen, D., Ring, A., Holzworth, R., and Krotkov, N.: Estimates of lightning NO<sub>x</sub> production based on OMI NO<sub>2</sub> observations over the Gulf of Mexico, *J. Geophys. Res.*, 121, 8668-8691, doi:10.1002/2015jd024179, 2016.
- Prather, M. J., and Jacob, D. J.: A persistent imbalance in HO<sub>x</sub> and NO<sub>x</sub> photochemistry of the upper troposphere driven by deep tropical convection, *Geophys. Res. Lett.*, 24, 3189-3192, doi:10.1029/97gl03027, 1997.
- Price, C., and Rind, D.: A simple lightning parameterization for calculating global lightning distributions, *J. Geophys. Res.*, 97, 9919-9933, doi:10.1029/92JD00719, 1992.
- 520 Price, C., and Rind, D.: What determines the cloud-to-ground lightning fraction in thunderstorms, *Geophys. Res. Lett.*, 20, 463-466, doi:10.1029/93gl00226, 1993.
- Price, C., and Rind, D.: Modeling global lightning distributions in a General-Circulation Model, *Mon. Weather Rev.*, 122, 1930-1939, doi:10.1175/1520-0493(1994)122<1930:Mglidia>2.0.Co;2, 1994.
- 525 Rap, A., Richards, N. A. D., Forster, P. M., Monks, S. A., Arnold, S. R., and Chipperfield, M. P.: Satellite constraint on the tropospheric ozone radiative effect, *Geophys. Res. Lett.*, 42, 5074-5081, doi:10.1002/2015gl064037, 2015.
- Reed, C., Evans, M. J., Di Carlo, P., Lee, J. D., and Carpenter, L. J.: Interferences in photolytic NO<sub>2</sub> measurements: explanation for an apparent missing oxidant?, *Atmos. Chem. Phys.*, 16, 4707-4724, doi:10.5194/acp-16-4707-2016, 2016.
- 530 Sauvage, B., Martin, R. V., van Donkelaar, A., Liu, X., Chance, K., Jaeglé, L., Palmer, P. I., Wu, S., and Fu, T. M.: Remote sensed and in situ constraints on processes affecting tropical tropospheric ozone, *Atmos. Chem. Phys.*, 7, 815-838, doi:10.5194/acp-7-815-2007, 2007.
- Schumann, U., and Huntrieser, H.: The global lightning-induced nitrogen oxides source, *Atmos. Chem. Phys.*, 7, 3823-3907, doi:10.5194/acp-7-3823-2007, 2007.
- 535 [Silvern, R. F., Jacob, D. J., Travis, K. R., Sherwen, T., Evans, M. J., Cohen, R. C., Laughner, J. L., Hall, S. R., Ullmann, K., Crouse, J. D., Wennberg, P. O., Peischl, J., and Pollack, I. B.: Observed NO/NO<sub>2</sub> ratios in the upper troposphere imply errors in NO-NO<sub>2</sub>-O<sub>3</sub> cycling kinetics or an unaccounted NO<sub>x</sub> reservoir." \*Geophysical Research Letters\* 45: 4466-4474.](#)
- Singh, H. B., Brune, W. H., Crawford, J. H., Jacob, D. J., and Russell, P. B.: Overview of the summer 2004 intercontinental chemical transport experiment - North America (INTEX-A), *J. Geophys. Res.*, 111, doi:10.1029/2006jd007905, 2006.
- 540 Singh, H. B., Brune, W. H., Crawford, J. H., Flocke, F., and Jacob, D. J.: Chemistry and transport of pollution over the Gulf of Mexico and the Pacific: spring 2006 INTEX-B campaign overview and first results, *Atmos. Chem. Phys.*, 9, 2301-2318, doi:10.5194/acp-9-2301-2009, 2009.
- Stettler, M. E. J., Eastham, S., and Barrett, S. R. H.: Air quality and public health impacts of UK airports. Part I: Emissions, *Atmos. Environ.*, 45, 5415-5424, doi:10.1016/j.atmosenv.2011.07.012, 2011.
- 545 Stratmann, G., Ziereis, H., Stock, P., Brenninkmeijer, C. A. M., Zahn, A., Rauthe-Schoch, A., Velthoven, P. V., Schlager, H., and Volz-Thomas, A.: NO and NO<sub>y</sub> in the upper troposphere: Nine years of CARIBIC measurements onboard a passenger aircraft, *Atmos. Environ.*, 133, 93-111, doi:10.1016/j.atmosenv.2016.02.035, 2016.
- Toon, O. B., Maring, H., Dibb, J., Ferrare, R., Jacob, D. J., Jensen, E. J., Luo, Z. J., Mace, G. G., Pan, L. L., Pfister, L., Rosenlof, K. H., Redemann, J., Reid, J. S., Singh, H. B., Thompson, A. M., Yokelson, R., Minnis, P., Chen, G., Jucks, K. W., and

- 550 Pszenny, A.: Planning, implementation, and scientific goals of the Studies of Emissions and Atmospheric Composition, Clouds and Climate Coupling by Regional Surveys (SEAC<sup>4</sup>RS) field mission, *J. Geophys. Res.*, 121, 4967-5009, doi:10.1002/2015jd024297, 2016.
- Tost, H., Jockel, P. J., and Lelieveld, J.: Lightning and convection parameterisations - uncertainties in global modelling, *Atmos. Chem. Phys.*, 7, 4553-4568, doi:10.5194/acp-7-4553-2007, 2007.
- 555 Travis, K. R., Jacob, D. J., Fisher, J. A., Kim, P. S., Marais, E. A., Zhu, L., Yu, K., Miller, C. C., Yantosca, R. M., Sulprizio, M. P., Thompson, A. M., Wennberg, P. O., Crounse, J. D., St Clair, J. M., Cohen, R. C., Laughner, J. L., Dibb, J. E., Hall, S. R., Ullmann, K., Wolfe, G. M., Pollack, I. B., Peischl, J., Neuman, J. A., and Zhou, X. L.: Why do models overestimate surface ozone in the Southeast United States?, *Atmos. Chem. Phys.*, 16, 13561-13577, doi:10.5194/acp-16-13561-2016, 2016.
- 560 van Geffen, J. H. G. M., Boersma, K. F., Van Roozendaal, M., Hendrick, F., Mahieu, E., De Smedt, I., Snee, M., and Veefkind, J. P.: Improved spectral fitting of nitrogen dioxide from OMI in the 405-465 nm window, *Atmos. Meas. Tech.*, 8, 1685-1699, doi:10.5194/amt-8-1685-2015, 2015.
- Worden, H. M., Bowman, K. W., Kulawik, S. S., and Aghedo, A. M.: Sensitivity of outgoing longwave radiative flux to the global vertical distribution of ozone characterized by instantaneous radiative kernels from Aura-TES, *J. Geophys. Res.*, 116, doi:10.1029/2010jd015101, 2011.
- 565 Ziemke, J. R., Chandra, S., and Bhartia, P. K.: "Cloud slicing": A new technique to derive upper tropospheric ozone from satellite measurements, *J. Geophys. Res.*, 106, 9853-9867, doi:10.1029/2000jd900768, 2001.